Journal of Physics: Conference Series

PAPER • **OPEN ACCESS**

A Control Algorithm of Active Wave Compensation System Based on the Stewart Platform

To cite this article: Huiyuan Wu *et al* 2023 *J. Phys.: Conf. Ser.* **2458** 012040

A Control Algorithm of Active Wave Compensation System Based on the Stewart Platform

Huiyuan Wu[1], Wenlin Yang[1]*, Muk Chen Ong[2], Tianhui Fan[3], Guang Yin[2], Weixiang Zeng[1], Weilun Situa[1], Yunting Wang[1]

[1.] Guangdong Institute of Intelligent Unmanned System, Guangzhou, China;

[2.] Department of Mechanical and Structural Engineering and Materials Science, University of Stavanger, Stavanger, Norway

[3.] School of Civil Engineering and Transportation, South China University of Technology, Guangzhou, China.

*Correspondence: yangwenlin@gis.sia.cn

Abstract. Aim at the actual engineering requirements of wind power operation and maintenance under complex sea conditions, a control method of the active wave compensation system for maintenance ships based on the Stewart platform is presented. The kinematics of the platform is analyzed, and the coordinate transformation, pose, and inverse solutions are analyzed and calculated. The multi-body dynamics simulation model is established by using MATLAB. For the problem of the load nonlinearity and strong coupling of the nonlinear Stewart platform, an active wave compensation active disturbance rejection control (ADRC) is built to attain the high-precision control of the six-degree-of-freedom (6-DOF) Stewart platform. The numerical simulation shows that the proposed control scheme has good tracking accuracy and strong anti-interference ability.

1. Introduction

In recent years, under the requirements of carbon peaking and carbon neutrality, the offshore wind power industry has received increasing attention. Wind power operation and maintenance are an important part of the industrial chain. It is also favored by the market[1-3]. However, offshore weather changes rapidly, the natural conditions are complex. Therefore, effective solutions need to be developed to address the difficult challenges of offshore wind operation and maintenance[4].

When the operation and maintenance ship sends professionals to the operation site, the ship will have six degrees of freedom movement under the influence of the Marine environment. If not handled properly, it is easy to have safety accidents[5]. The boarding trestle has a relatively large movement under high sea conditions, which will cause serious safety hazards to the boarding operators. To ensure the safety of personnel, the ship needs to be equipped with a device that can actively compensate the six degrees of freedom motion. Compared with the ordinary gangway, the active wave compensation trestle can remain relatively stable under complex ocean conditions, meeting the safety requirements of personnel boarding, leaving the wind tower, and effectively extending the operation and maintenance window period[6].

However, the control system of the active wave compensation trestle has problems such as large inertia, large time delay, and multi-parameter coupling[7-9]. In response to these problems, engineers and technicians have carried out a lot of research work. In some studies[10], a solution using wave compensation value was proposed, and a compensation device based on a micro inertial navigation sensor was designed. Aim at decreasing the influence of sea wind and waves on ship operation and maintenance, a wave compensation platform was proposed[11]. A boarding trestle with an active compensation function was explored to meet the commuting needs of operation and maintenance under high sea conditions[12]. An intelligent pseudo-differential control algorithm was studied to overcome the influence of wind and waves[13]. The author improved the particle swarm method to enhance the controller parameters of the wave compensation control system[14]. In this paper, a parallel 6-DOF Stewart platform is selected as the compensation device. The platform is a nonlinear system with complicated coupling relationship between inputs and outputs[15-17]. And the traditional PID algorithm is difficult to meet the control requirements in the face of nonlinear systems. For the problem of parameter uncertainty and unknown interference in the Stewart platform, a sliding mode control method with a boundary layer was presented[18]. ADRC has great advantages in dealing with nonlinear systems and has been favored by researchers. The authors designed a permanent magnet synchronous motor servo control system by combining ADRC with PID control[19]. A strategy of combining a new nonlinear function and an extended state observer to form an ADRC system was designed to overcome the problem of low control accuracy for coal mine robots working in complex coal mine environments[20].

However, there is still a lack of research on applying ADRC to the active wave compensation control of the 6-DOF Stewart platform with nonlinear characteristics. The Stewart platform is adopted in this paper to meet the engineering requirements of the ship in the course of operation. The active wave compensation mechanism of the boarding trestle adopts the ADRC method to realize the tracking control of the 6-DOF platform. The result of simulation show the tracking effectiveness and robustness of the strategy.

The remainder of this article is organized as follows. In section 2, the kinematic analysis of the Stewart platform is described. Section 3 presents the single-channel model of hydraulic servo channels. In section 4, the controller is designed. In section 5, a simulation is conducted to verify the effectiveness of the proposed control, and a summary is provided in section 6.

2. KINEMATIC ANALYSIS OF THE STEWART PLATFORM

2.1. Position and attitude description of the platform

The model of the 6-DOF Stewart platform is displayed in Figure 1. The platform includes an upper platform, a lower platform, an upper and lower Hooke hinge, a servo actuator, and a base. The servo actuator receives the control signal of the servo control system and drives the electric cylinder or hydraulic cylinder to move. The upper platform can realize the movement in the roll, pitch, yaw, X, Y, and Z directions, thus providing six degrees of freedom motion compensation for the active wave compensation boarding trestle installed on the upper platform.

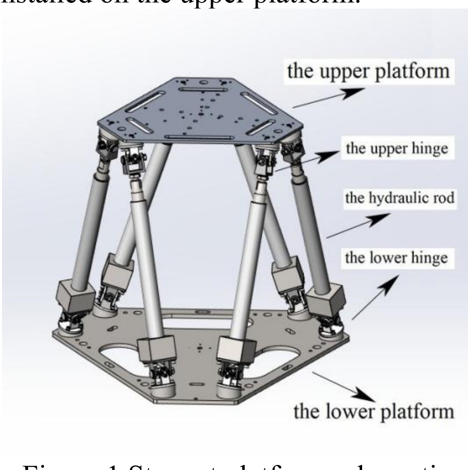

Figure 1 Stewart platform schematic

The platform coordinate system is established to show the mobile platform's position and altitude, as shown in Figure 2. A static coordinate system {B} $(O_b - X_b Y_b Z_b)$ is settled on the base and a dynamic coordinate system {P}$(O_p - X_p Y_p Z_p)$ on the upper platform. The position description of the Stewart platform is represented by the relative position of the moving coordinate system of the upper platform relative to the static coordinate system of the base. It is expressed as $t = [X_1, Y_1, Z_1]^T$. Where, X_1 , $Y_1$and Z_1 represent the longitudinal, lateral, and vertical motions of the mobile platform relative to the static coordinate system respectively. The altitude of the platform is described by the method of rotating the coordinate system. The Euler angle $[\phi, \theta, \psi]^T$ are obtained by three consecutive rotations of the upper platform, among which $\phi,\ \theta,\ and\ \ \psi$ respectively define the rolling, pitching, and yaw rotational motions of the platform around the three axes of the static system. The rotation matrix can be obtained according to the following equations.

$$R = \begin{bmatrix} c\psi c\theta & c\psi s\theta s\phi - s\psi c\phi & s\psi s\phi + c\psi s\theta c\phi \\ s\psi c\theta & c\psi c\phi + s\psi s\theta s\phi & s\psi s\phi c\phi s\phi \\ -s\theta & c\theta s\phi & c\theta c\phi \end{bmatrix} \quad (1)$$

Where, *s* = *sin*, and *c* = *cos*.

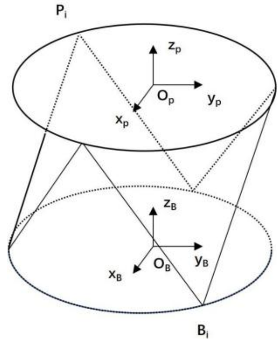

Figure 2 Schematic diagram of platform coordinates

2.2. Position inverse analysis

In the case of obtaining the parameters of the platform structure and the position and altitude of the upper platform, the process of solving the telescopic lengths of all its driving mechanisms belongs to the inverse solution process of solving the kinematics of the 6-DOF platform. According to the geometric significance, the vector of the driving mechanism can be expressed to analyze the *i* platform drive mechanism shown in Figure 3.

$$\vec{l_i} = R\vec{d_i} + \vec{t} - \vec{b_i} (i = 1, \ldots, 6) \quad (2)$$

Among them, *d* represents the coordinates of the hinge points of each driving mechanism in the moving coordinate system, and *b* represents the coordinates of the lower hinge points of each driving mechanism in the static coordinate system. The length of the driving mechanism can be from the Euclidean norm.

$$\|\vec{l_i}\| = \left(\vec{l_i}^T \vec{l_i}\right)^{\frac{1}{2}} \quad (3)$$

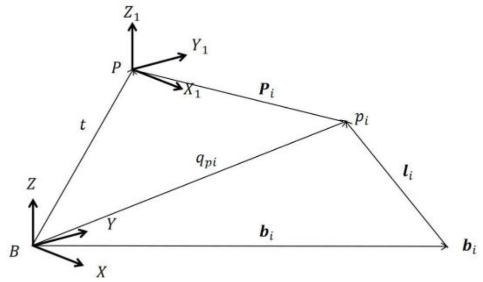

Figure 3 Position Analysis of Drive Mechanism

3. ACTIVE DISTURBANCE REJECTION CONTROLLER

For high-frequency signals, the ADRC has designed a transition process method, which is similar to low-pass filtering a given command to obtain an easier-to-implement command, thereby greatly reducing overshoot while sacrificing part of the rapidity. In the PID controller, one of the main functions of the integral is to eliminate disturbances, but the integral works relatively slowly and can also cause an overshoot. To improve this shortcoming, the ADRC uses an extended state observer to observe target. The estimated value is used as compensation to cancel out the interference. The traditional linear feedback method has shortcomings in the convergence speed and anti-interference ability. Active disturbance rejection control replaces the traditional gain with a nonlinear function and replaces the linear feedback with nonlinear feedback. There are six driving mechanisms on the 6-DOF platform, and the control principles of these six driving mechanisms are the same. The control algorithm of the ADRC controller is as follows.

(1) The tracking differentiator (TD) for the transition process is as follows.

$$v_1(k+1) = v_1(k) + hv_2(k) \tag{4}$$

$$v_2(k+1) = v_2(k) + hfst(v_1(k) - v_0(k), v_2(k), r, h_0) \tag{5}$$

The output v_1 of the TD tracks the input *v*. And v_2 tracks the differential of *v*. The parameters that need to be tuned include the speed factor *r*, the integration step size *h,* and the filter factor h_0. And the function $fst(v_1(k) - v_0(k), v_2(k), r, h_0)$ is expressed as follows.

$$fst(x_1, x_2, r, h) = -\begin{cases} rsgn(a), |a| > b \\ r\dfrac{a}{d} \quad , |a| < d \end{cases} \tag{6}$$

Where, sgn is a symbolic function, and a and d can be designed.

$$a = \begin{cases} x_2 + \dfrac{a_0 - d}{2} sgn(y), |y| > d_0 \\ x_2 + \dfrac{y}{h}, |y| < d_0 \end{cases} \tag{7}$$

$$\begin{cases} d = rh \\ d_0 = hd \\ y = x_1 + hx_2 \\ a_0 = (d^2 + 8r|y|)^{\frac{1}{2}} \end{cases} \tag{8}$$

(2) The extended state observer is used.

$$\begin{cases} \varepsilon = z_1(k) - y(k) \\ z_1(k+1) = z_1(k) + h[z_2(k) - \rho_1 \varepsilon] \\ z_2(k+1) = z_2(k) + h[z_3(k) + \rho_2 fal(\varepsilon, a_1, \delta) + b_0 u(k)] \\ z_3(k+1) = z_3(k) + h\rho_3 fal(\varepsilon, a_1, \delta) \end{cases} \tag{9}$$

Among them, ρ_1, ρ_2, and ρ_3 are called system error correction gains, which are the observer coefficients of extended state observer. Selecting appropriate parameters can well estimate the disturbance. The expression of the function *fal*() is established below.

$$fal(\varepsilon, a_1, \delta)\begin{cases} |\varepsilon|^{a_1} + sgn(\varepsilon), |\varepsilon| > \delta \\ \dfrac{\varepsilon}{\delta^{1-a_1}}, |\varepsilon| < \delta \end{cases} \tag{10}$$

(3) The nonlinear state error feedback is given.

$$\begin{cases} e_1 = v_1(k) - z_1(k) \\ e_2 = v_2(k) - z_2(k) \\ u_0 = \rho_1 fal(e_1, a_1, \delta) + \rho_2 fal(e_2, a_2, \delta) \\ u(k) = u_0(k) - \dfrac{z_3(k)}{b_0} \end{cases} \tag{11}$$

Where, u_0 is the control quantity, $u(k)$ is the total output, and z_3 is the disturbance estimator in the control system.

4. Simulation analysis

The structure sketch map of the simulation system is displayed in Figure 4. The desired pose of the moving platform is obtained according to the desired trajectory, and the desired displacement of each driving mechanism paired with the desired trajectory of the upper platform is obtained by the inverse kinematics solution. Then the expected displacement, actual displacement, and speed of each driving mechanism are used as the input of the controller. And the output of the controller is the force acting on each driving mechanism.

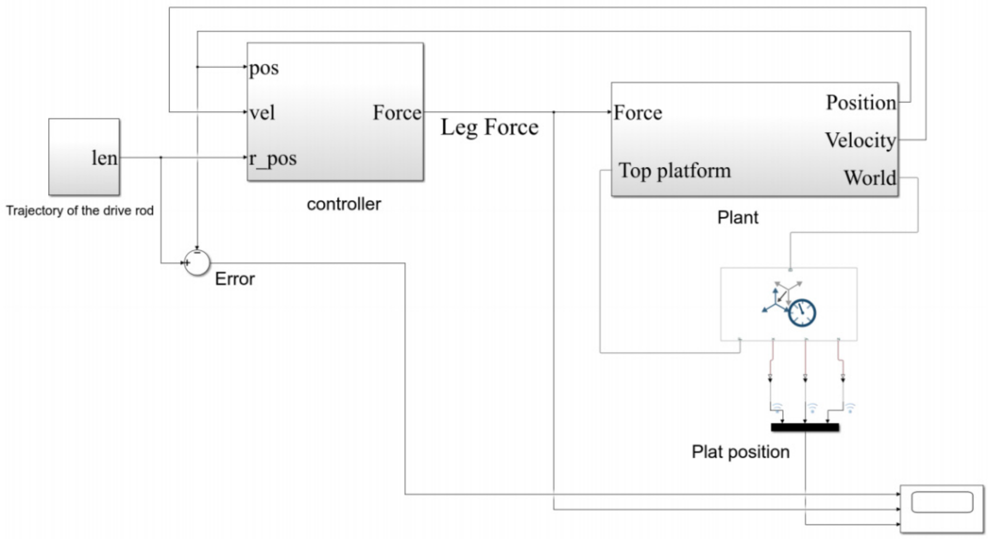

Figure 4 Simulation system block diagram

The driving mechanism structure is described below. The upper and lower ends are linked to the upper and lower platforms by a Hook hinge. There is a hydraulic cylinder in the middle of the rod that connects the upper and lower parts of the rod. As the upper platform moves, causing the length of the rod to change and the sensor to measure the displacement and speed of the rod.

Figure 5 shows the tracking trajectories of the six driving mechanisms using the ADRC method, where, the abscissa is time, the ordinate is the drive mechanism displacement, the blue lines are the desired trajectory, and the red lines are the actual trajectory. Figure 6 demonstrates the tracking error of the driving mechanism by using the ADRC algorithm, and the tracking error is close to zero. It can be seen that the ADRC method can obtain high-precision tracking performance.

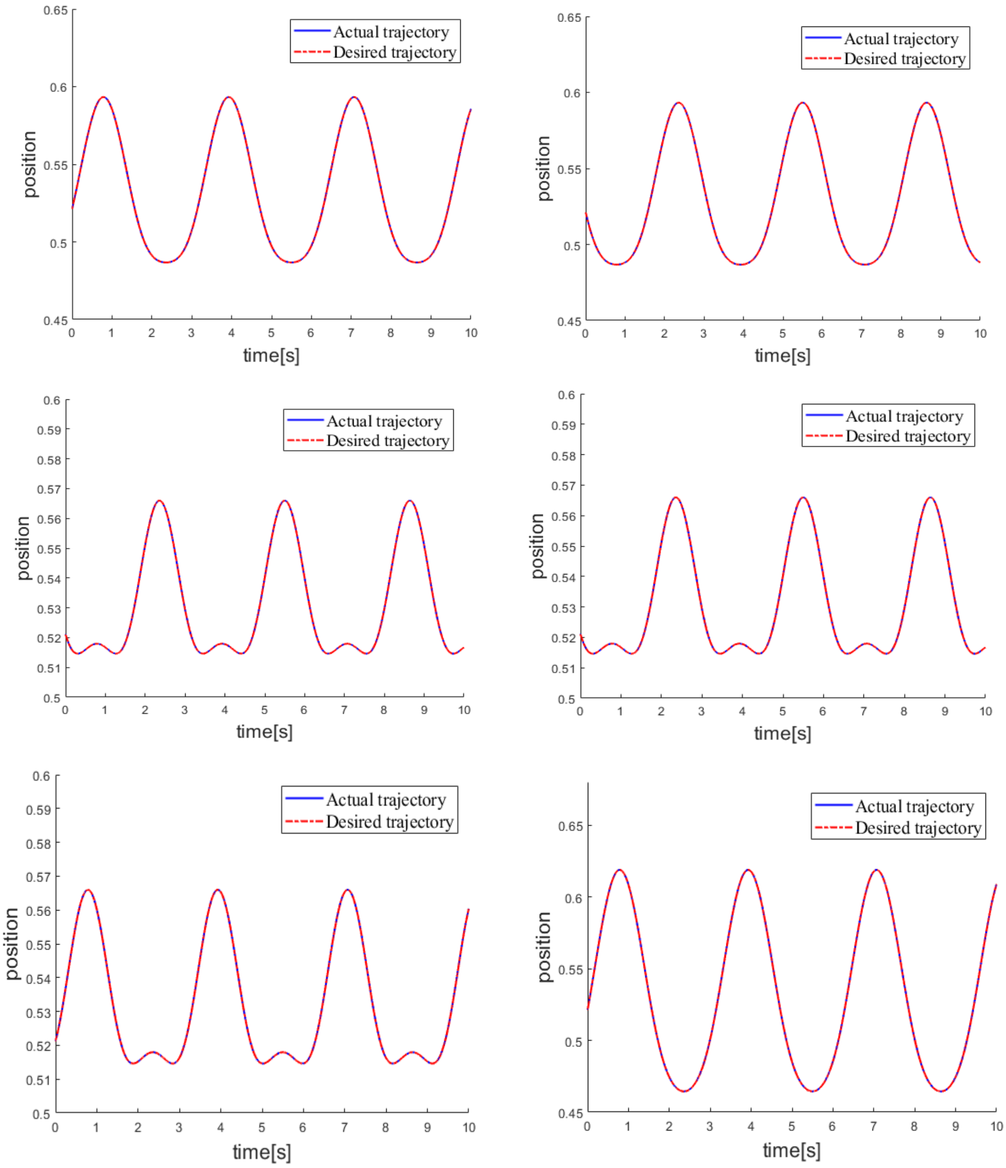

Figure 5 Trajectory tracking graph using ADRC

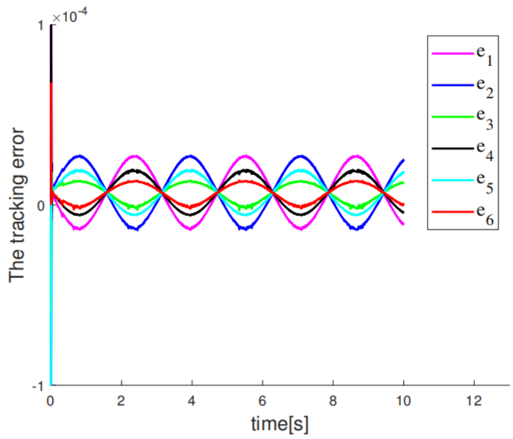

Figure 6 Tracking error plots using ADR

5. CONCLUSION

In this paper, a 6-DOF active wave compensation control algorithm of marine operation and maintenance ship boarding trestle based on the Stewart platform is developed and studied. Firstly, the kinematics analysis and calculation of the Stewart platform are carried out through MATLAB/ Simulink. Secondly, based on the nonlinearity and strong coupling problems of the Stewart platform and combined with the active wave compensation automatic disturbance rejection control algorithm, a six-degree-of-freedom active wave compensation simulation experiment was carried out. The simulation experiments show that the active wave compensation active disturbance rejection control strategy has excellent tracking property and well anti-interference ability, which offers an effective solution for the high-precision active wave compensation control of wind power operation and maintenance ship boarding trestle bridges.

Acknowledgments

This work was supported in part by the International Science and Technology Cooperation Project of Guangdong Province under Grant 2022A0505050027, and the Provincial Basic and Applied Basic Research Fund Project of Guangdong Province under Grant 2021A1515012552.

References

[1] X. Yibo. Research on the watertight performance of offshore wind turbines. *Nanfang Agricultural Machinery* 2022.
[2] L. Yang, G. Li, Z. Zhang, X. Ma, and Y. Zhao. Operations and maintenance optimization of wind turbines integrating wind and aging information. *IEEE Transactions on Sustainable Energy*; 2021; pp. 211-221.
[3] A. Kisvari, Z. Lin, and X. Liu. Wind power forecasting a data-driven method along with the gated recurrent neural network. *Renewable Energy*; 2021; pp. 1895-1909.
[4] K. Y. Yan Xu and G. Zhao. The influencing factors and hierarchical relationships of offshore wind power industry in china. *ENVIRONMENTAL SCIENCE AND POLLUTION RESEARCH*; 2021; pp. 329-344.
[5] M. Li, X. Jiang, and R. R. Negenborn. Opportunistic maintenance for offshore wind farms with multiple-component age-based preventive dispatch. *Ocean Engineering*; 2021; pp. 109-115.
[6] L. Tang and Y. Chen. Dynamic model of four degrees of freedom rope-driven rigid-flexible hybrid wave compensation device. *Journal of Mechanical Science and Technology*; 2020; pp. 1937-1948.
[7] S. F. Lu Dongqing. Simulation Research on Active Wave Compensation Control Technology. *Ship*; 2012.
[8] C. Y. Chen. An Wanping, Research on hydraulic control principle of active wave compensation based on boarding trestle. *Equipment Manufacturing Technology*; 2019.
[9] J. Leng, C. Xu, M. Li, H. Du, and S. Liu. Control strategy for performing predictions for a semi-active compensation system. *Ocean Engineering*; 2021; pp. 137-148.
[10] G. W. Lu Daohua. Design and Simulation of Active Wave Compensation Platform and Its Test System. *Ship Engineering*; 2015.
[11] H. C. Tang Gang. Modeling and Simulation of Three-DoF Parallel Wave Compensation Platform. *journal of Shanghai Maritime University*; 2020.
[12] Z. W. Su Changqing. An active wave compensation method for boarding trestle bridges. *Ship and Ocean Engineering*; 2017.
[13] M. X. Yan Hualin. Application of Active Wave Compensation in Position Control System. *Manufacturing Automation*; 2017.
[14] T. G. P. Control system research in wave compensation based on particle swarm optimization. *Scientific Reports*; 2021.
[15] C. H. Zhou Ting. Electro-hydraulic servo six-degree-of-freedom composite loading device control system. *Modern Manufacturing Engineering*; 2021.

[16] Y. Cai, S. Zheng, W. Liu, Z. Qu, J. Zhu, and J. Han. Sliding-mode control of ship-mounted Stewart platforms for wave compensation using velocity feedforward. *Ocean Engineering*; 2021.
[17] Y. Cai, S. Zheng, W. Liu, Z. Qu, J. Zhu, and J. Han. The adaptive robust dual-loop control scheme of ship-mounted Stewart platforms for wave compensation. *Mechanism and Machine Theory*; 2021.
[18] T. L. Hu Yongpan. Robust control method for parallel wave compensation system. *Journal of National University of Defense Technology*; 2014.
[19] H. L. Wang Zhida. An active wave compensation method for boarding trestle bridges. *Computer and Digital Engineering*; 2022.
[20] J. X. Xu Weifeng. Research on Active Disturbance Rejection Control of Coal Mine Robot Trajectory Tracking. *Coal Mining Machinery*; 2021.